

DETC2013-13086

MICROSURGICAL DEVICES BY POP-UP BOOK MEMS

Joshua B. Gafford

Dept. Engineering and Applied Sciences
Harvard University
Cambridge, MA 02138
Email: jgafford@seas.harvard.edu

Samuel B. Kesner

Technology Development Fellow
Wyss Institute, Harvard University
Cambridge, MA 02138
Email: samuel.kesner@wyss.harvard.edu

Robert J. Wood

Charles River Professor of Engineering and
Applied Sciences, Harvard University
Core Faculty Member, Wyss Institute
Cambridge, Massachusetts 02138
Email: rjwood@seas.harvard.edu

Conor J. Walsh

Assistant Professor of Mechanical and Biomedical
Engineering, Harvard University
Core Faculty Member, Wyss Institute
Cambridge, Massachusetts 02138
Email: walsh@seas.harvard.edu

ABSTRACT

The small scale of microsurgery poses significant challenges for developing robust and dexterous tools to grip, cut, and join sub-millimeter structures such as vessels and nerves. The main limitation is that traditional manufacturing techniques are not optimized to create smart, articulating structures in the 0.1 – 10 mm scale. Pop-up book MEMS is a new fabrication technology that promises to overcome this challenge and enable the monolithic fabrication of complex, articulated structures with an extensive catalog of materials, embedded electrical components, and automated assembly with feature sizes down to 20 microns. In this paper, we demonstrate a proof-of-concept microsurgical gripper and evaluate its performance at the component and device level to characterize its strength and robustness. 1-DOF Flexible hinge joints that constrain motion and allow for out-of-plane actuation were found to resist torsional loads of 22.8 ± 2.15 N-mm per mm of hinge width. Adhesive lap joints that join individual layers in the laminate structure demonstrated a shear strength of 26.8 ± 0.53 N/mm². The laminate structures were also shown to resist peel loads of 0.72 ± 0.10 N/mm². Various flexible hinge and adhesive lap components were then designed into an 11-layered structure which ‘pops up’ to realize an articulating microsurgical gripper that includes a cable-driven mechanism for gripping actuation and a flexural return spring to passively open the gripper. The gripper prototype, with final weight of 200 mg, overall footprint of 18 mm by 7.5 mm, and features as

small as 200 microns, is able to deftly manipulate objects 100 times its own weight at the required scale, thus demonstrating its potential for use in microsurgery.

INTRODUCTION

Small joint surgery, such as that in the wrist or fingers, presents a number of significant challenges due to the limited maneuverable workspace and the presence of many delicate structures that must be avoided, including sensitive cartilage surfaces and tendons [1]. Current commercial small-joint surgical instruments are limited to straight, simple tools without any distal articulation which would allow for greater access and dexterity inside the joint [2]. In addition, the robust electromechanical surgical tools at the sub-mm scales required for these procedures are either impossible or commercially impractical to make with existing manufacturing techniques such as surface/bulk micromachining [3], wire-EDM [4], micro-injection molding, or micromilling/lathing [5]. It is our goal to apply an emerging micromachining and assembly technique that we have developed to enable robust, dexterous, and practical microsurgical instruments for small joint repair.

We have developed a novel micro-manufacturing technique known as Pop-Up Book MEMS (‘Pop-Ups’) that allows for the fabrication of complex, multi-functional electromechanical devices on the 0.1-10 mm scale [6] [7]. Pop-Up technology enables the ability to create 3-D, multi-material, monolithic meso and micro-structures using purely 2-D planar

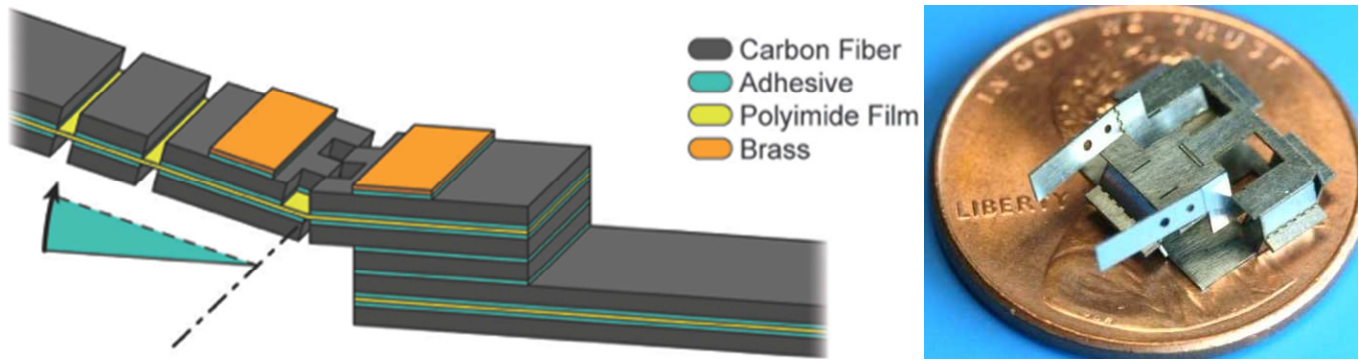


Figure 1: (left) Layup detail of a hinge created with the Pop-Up Book MEMS fabrication technology [1], (right) Device fabricated using Pop-Up Book MEMS, on a US penny for scale

manufacturing and origami folding techniques. The method draws upon techniques from printed circuit (PC) board manufacturing, allowing for the straightforward integration of embedded on-board electronics and power. An example Pop-Up mechanism, featuring a castellated hinge which allows the top structural layer to fold in on itself to approximate pin joint motion, is shown in Figure 1 (left).

Pop-Up Book MEMS technology is well-suited for small medical and microsurgical applications, as the technique enables the manufacture of highly capable and articulated mechanisms at sub-mm scales. An early example of a self-assembling device manufactured via PopUp MEMS is shown in Figure 1 (right). The nature of PopUp devices will enable mechanisms and implants that can be inserted through small incisions and ‘pop-up’ to assume their functional form. Embedded sensing and actuation can be directly integrated into the end-effector to allow for distal actuation and feedback sensing in teleoperative and cooperative robotic scenarios.

While great innovations have been created with Pop-Up fabrication, such as flying microrobots or self-assembling structures [7], no work to date has been done to mechanically characterize the strength and robustness of Pop-Up devices. As our objective is to build devices that will mechanically interact with the human anatomy, it is crucial to understand the forces that these devices can withstand to ensure functional longevity in a mechanically interactive environment. In the following paper, we begin with an overview of the Pop-Up Book MEMS manufacturing process. We provide a discussion of the robustness evaluation experimental methods and present significant results of the evaluation. Finally, we present the design, fabrication, and evaluation of an actuated gripper prototype developed using Pop-Up MEMS.

POPUF FABRICATION PROCESS

Mechanisms created with the Pop-Up technology are typically composed of a number of layups consisting of five sub-layers: a flexible (polyimide) layer sandwiched between two structural layers, with adhesive in between each layer (see Figure 1). The number of layers scales roughly with device complexity. In this work, 304 Stainless Steel is used as the

structural material, and Kapton® (developed by DuPont) is used as the flexible polyimide. Dupont FR1500 acrylic adhesive is used to join the layers.

An overview of the fabrication process is illustrated Figure 2. Beginning with a 2D CAD model of the device, interior and alignment features on each individual layer comprising the layup are machined via laser ablation using a diode-pumped solid-state (DPSS) laser. Each layer is then deburred if necessary and exposed to a two-step cleaning process: (1) Isopropyl Alcohol soak and ultrasonic clean (80° C for 10 minutes) to remove surface-level particulates, and (2) plasma etch with argon gas (0.40 mbar at 2-4 sccm for 60s [8]) to remove contaminants and improve the surface microtexture. The layers are then prepped for lamination and each structural layer is ‘back-tacked’ to deposit the adhesive islands on each respective layer such that the adhesive protective backing can be removed and disposed of. The entire laminate is cured via a two-hour curing process where heat and pressure (60 psi, 200° C) are applied to set the adhesive. Following this step, the layup is released from the surrounding alignment scaffold using the DPSS laser and mechanically ‘popped up’ to assume the functional form of the prototype. From start to finish, the entire fabrication process takes approximately 10 hours.

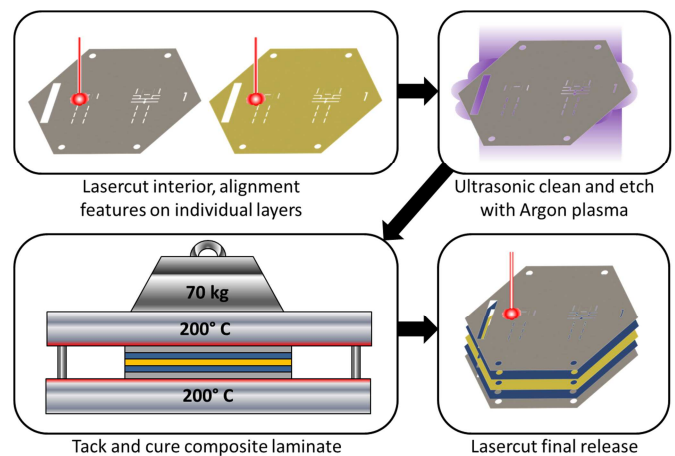


Figure 2: Pop-Up manufacturing process illustration

COMPONENT DESIGN AND EVALUATION

Further development of PopUp technology with specific application to medical devices and microsurgical equipment requires a thorough understanding of the forces that PopUp structures can withstand. The technology was originally developed for flying microrobots, so strength-to-weight ratio optimization was key. As such, limited work has since been done to characterize the strength and robustness of these structures as this had not previously been a primary design consideration. As we are developing mechanisms that will manipulate and interact directly with soft-tissue, we performed a robustness analysis to mechanically characterize the technology and improve our understanding of the strength capabilities of Pop-Up structures at sub-millimeter scales. This work will guide future manufacturing process optimization and design projects.

EXPERIMENTAL METHOD

To evaluate the robustness of the Pop-Up fabrication process, a subset of frequently used components had their strength properties measured and failure modes examined. These failure modes are: (1) lap shear failure resulting in adhesive delamination (layouts both with and without the flexible Kapton layer), (2) delamination via peel failure, and (3) castellated hinge failure via torsional loading. A custom aluminum jig with an elastic hinge, capable of friction clamping components $<500 \mu\text{m}$ thick, was fabricated so that the small specimens could be evaluated using a standard material tensile testing machine (Instron Model 5566 with 1 kN static load cell). Illustrations of each strength test, as well as images of test specimens undergoing testing, are shown Figure 3. Lap shear samples featured an overlapping area of adhesion to resist shear forces, as per the ASTM protocol set forth in [9]. Lap peel samples were of similar design, except with perpendicular tabs to obtain a pure peeling motion. Hinge samples featured a castellated hinge with a 10mm lever arm to provide a bending moment about the hinge.

For each failure mode, a meaningful parameter was varied to obtain trend data for use as scaling guidelines in future mechanism design. For lap shear and peel failure modes, lap area of adhesion was varied (1mm^2 , 3mm^2 , and 5mm^2 for lap shear; 3mm^2 , 9mm^2 , and 15mm^2 for peel). For castellated hinge torsion, hinge width was varied (1mm, 3mm, and 5mm).

Five specimens were tested for each varied parameter to obtain a statistically meaningful dataset with which to compute confidence intervals. Given 3 variables for 4 tests, a total of 60 tests were performed to characterize the robustness of the technology.

ROBUSTNESS RESULTS

Raw instron data from each experiment were recorded. In addition, a representative sample from each test was further analyzed under a scanning electron microscope (SEM) to examine any significant qualitative observations regarding the failure mode. An example raw force/extension curve generated

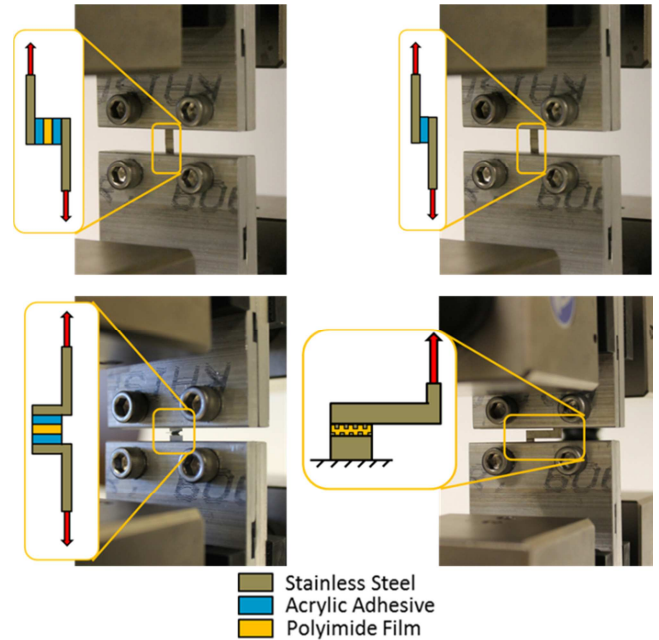


Figure 3: PopUp strength test specimens (clockwise from top left) Steel-Kapton-Steel Lap Shear, Steel-Steel Lap Shear, Castellated Hinge Torsion, Steel-Kapton-Steel Lap Peel

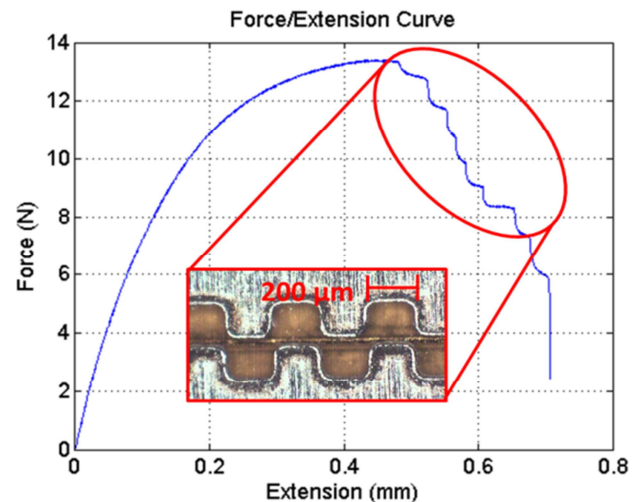


Figure 4: Test data for castellated hinge torsion, demonstrating effects of stress concentrations inducing failure. Inset shows microscopic image of castellated hinge pre-test

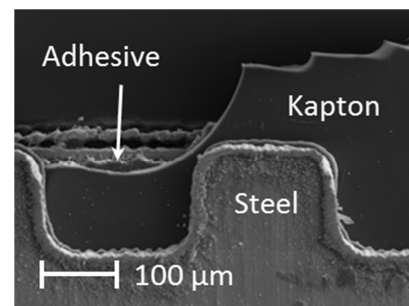


Figure 5: SEM image of Kapton failure at castellation

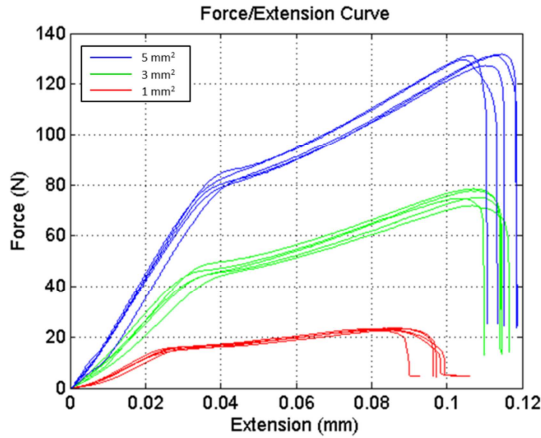


Figure 6: Example results of Steel-Kapton-Steel lap shear failure, demonstrating effects of increasing lap area

from the castellated hinge torsion failure evaluation is shown in Figure 4. The inlaid image is an optical microscopic image of the castellated region pre-testing. In addition, an SEM close-up of the failure region for this sample is shown in Figure 5.

Aggregate loading curves for Steel-Kapton-Steel lap shear evaluation for the three different lap areas (15 samples) are shown in Figure 6. Loading curves were relatively consistent and devoid of statistical outliers, and scale approximately linearly with lap area, as was hypothesized. Similar trends were observed with Steel-Steel lap shear, Steel-Kapton-Steel lap peel and castellated hinge torsion evaluations.

Raw data were post-processed in MATLAB (Mathworks, Natick, MA, USA) and a statistical analysis was performed. Failure modes of interest were plotted against the varied parameter for that particular test, and linear regression was performed to obtain strength data as a function of the feature size. Standard measurement errors in slope were computed using a least-squares approach with 95% confidence assuming a student-t distribution of data [10].

Linear fits for each dataset are given in Figure 7 (a), (b), and (c). The results are tabulated in Table 1. Data analysis indicates that trends are sufficiently linear; peel strength data

Table 1: Robustness results summary. \pm values denote 95% confidence intervals

Property	Layup	No. Samples	Value	Units
Shear Strength (per unit area)		15	26.8±0.53	N/mm ²
Shear Strength (per unit area)		15	22.1±1.60	N/mm ²
Peel Strength (per unit area)		15	0.72±0.10	N/mm ²
Hinge Torsional Strength (per unit width)		15	22.8±2.15	N

has the largest 95% confidence interval, comprising roughly 13% the magnitude of the fitted linear function. The remaining tests had confidence intervals to within 10%, demonstrating sufficient statistical confidence in the results. Note that, in the case of hinge torsional failure, a power fit minimizes the residual, but the trend is sufficiently linear in the region of interest.

DISCUSSION

Results generated from the robustness evaluation are extremely encouraging. We have demonstrated that PopUp components can withstand appreciable shear and torsional forces, and have quantified these failure modes in the interest of guiding future manufacturing process optimization and Pop-Up mechanism design work. The absence of outliers speaks to process and manufacturing consistency which is promising as the fabrication process is not performed in a cleanroom.

An interesting phenomenon was observed upon further inspection of the castellated hinge torsional failure results, demonstrated in the example empirical results shown in Figure 4. Observe the step-like pattern in the torque/extension under high stress. This occurs because the corners of the steel castellations pierce the Kapton layer, resulting in failure. This effect is further highlighted in the SEM closeup shown in Figure 5. The sawtooth-like pattern of the failed Kapton evident in Figure 5 has edges that roughly align with corners of the

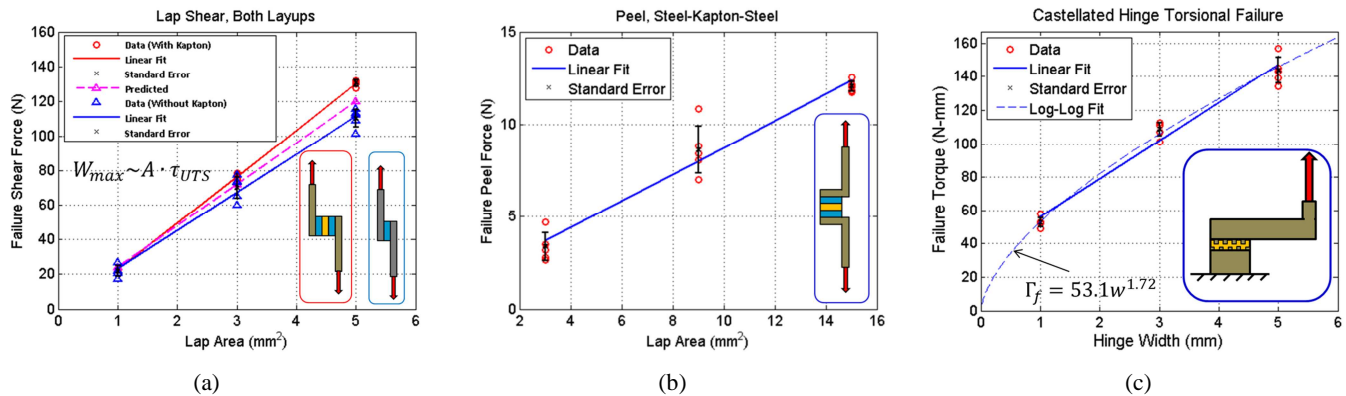


Figure 7: (a) Lap Shear Failure test results (data and linear fit) for Steel-Steel layup (Red) and Steel-Kapton-Steel (blue) layup, with predicted failure profile given ultimate shear strength of acrylic adhesive, (c) Peel failure test results, (c) Castellated hinge torsion failure test results (data, linear and power fit)

castellations, implying failure due to stress concentrations induced by the castellations. In addition to visual evidence, audible cues were present during testing (sequential ‘popping’ noises immediately before ultimate failure) implying the same conclusion. Based on this insight, castellation corners examined in this work were given a 50 μm curvature radius, and torsional strength more than doubled over unrounded castellated hinges in previous designs as the stress concentrations induced on the Kapton film were significantly reduced.

Another interesting result from the post-processed data, illustrated in Figure 7(a), is that the lap shear samples with the Steel-Steel laminate performed worse than those with the Steel-Kapton-Steel laminate. This result indicates that the inclusion of the Kapton intermediate layer actually improves layup adhesion and shear resistance. It also indicates that the quality of adhesion improves proportionally with the amount of Kapton present, given by the difference in slope. The theory behind this is that exposure to argon plasma improves the surface energy of Kapton, thereby improving its overall adhesive properties [11]. Argon-treated Kapton has a larger polar surface energy component (~ 60 mN/mm) than argon-treated 304 Stainless steel (~ 50 mN/mm) [11] [12]. Since acrylic adhesive is polar by nature, Kapton forms a stronger bond with the adhesive than the steel, which must rely on weaker dispersive (Van-Der-Waals) bonds. This is a possible explanation for the slope discrepancy observed in Figure 7 (a).

Overall, the magnitudes of shear resistance and hinge torsional resistance are far beyond *a priori* postulations. For comparison, given a yield strength of $\sigma_y = 520$ MPa for stainless steel, the tensile stress (stress normal to the cross-section) in a 5mm wide by 50 μm thick stainless steel coupon with a 5mm² lap area is 518 MPa at lap shear failure. Thus, the shear resistance of the adhesive joint is approximately as strong as the tensile strength of the steel itself. It is observed that peel failure is the weakest link, but compensatory design work can be undertaken to ensure that this failure mode never happens in practice, including interlocking structural elements to prevent overextension. The linear trend computed for each mechanism will allow for mechanism scaling in future design work once design forces and loads are determined.

MICROSURGICAL GRIPPER CONCEPT

In order to demonstrate the feasibility of PopUp MEMS for developing miniature medical devices, the manufacturing process outlined previously was used to develop a microsurgical gripper prototype that includes a number of the adhesive lap joints and hinge joints evaluated in the previous Section. The prototype was designed with a form-factor (1mmx10mm gripper jaws) consistent with microsurgery requirements in an effort to fabricate a gripper for the robotic work presented in [13]. The gripper was designed with cable-driven actuation for the closing mechanism and a flexural spring that applies a restoring force to passively open the gripper. A conceptual image of the gripper prototype is shown in Figure 8.

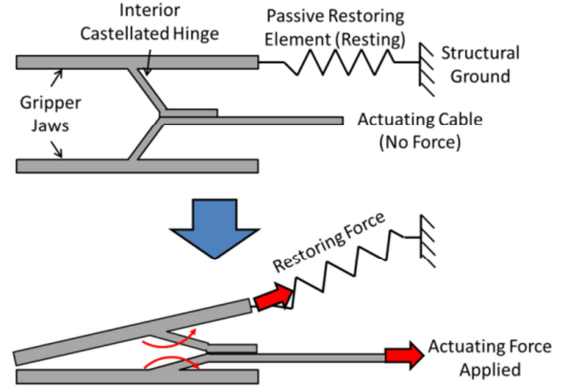


Figure 8: Microsurgical gripper functional illustration

PASSIVE RETURN DESIGN

In designing the passive return, a tradeoff exists between gripper closing range-of-motion (spring compliance) and restoring force (spring stiffness), so serpentine springs were evaluated empirically and analytically for both of these characteristics. The spring is in its resting state when the mechanism is popped open, and would deform out of plane when actuated to provide a restoring force when the actuating force is removed. The complicated behavior of the spring deformation (out-of-plane, as demonstrated Figure 9) warrants a more rigorous analysis than simple first-principles.

The spring return was designed using a quasi-analytical process with empirical validation. The stiffness characteristics were approximated via an analytical model of serpentine springs (out-of-plane deflection, as in side view in Figure 9) to obtain order-of-magnitude flexural behaviors [14].

δ_z	Deformation in z-direction
E	Young's modulus of 304 SS steel
F	Applied force
G	Shear modulus of 304 SS steel ($= E/2(1 + \nu)$)
I_{y_o}	Second moment of area
J_o	Torsional moment of inertia
K_{δ_z}	Out-of-plane stiffness, z-direction
l_o	Minor length
l_p	Major length
N	Number of turns

$$K_{\delta_z} \sim \frac{6EI_{y_o}GJ_o}{(N+1)l_o^3GJ_o + (16N^3 + 36N^2 + 43N + 3)l_p^2l_oEI_{y_o}} \quad (1)$$

$$\delta_z \sim \frac{F}{K_{\delta_z}} \quad (2)$$

Several spring designs were fabricated and characterized empirically in a tensile testing (Instron) device to verify the analytical approximation. Example behaviors of two disparate flexure designs are shown in Figure 10. The results demonstrate excellent agreement (less than 10% spring constant error in both cases) between the estimated (Eq. 1) and empirical results in the

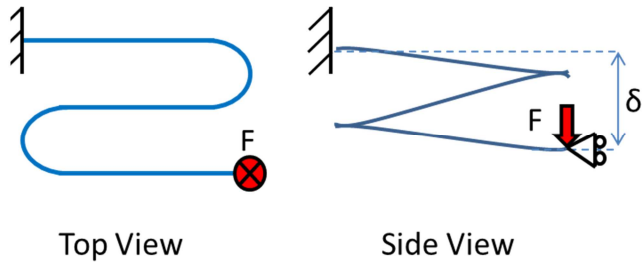


Figure 9: Illustration of serpentine spring pattern, demonstrating out-of-plane deflection

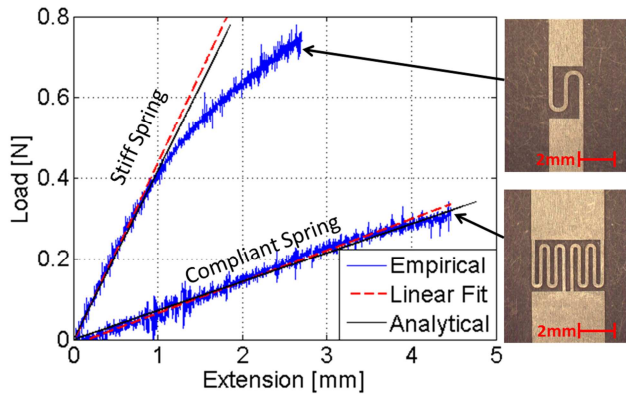


Figure 10: Analytical and experimental behavior of stiff (low compliance, high restoring force) and soft (high compliance, low restoring force) passive flexural elements

linear region of spring operation. Once the load/displacement curve becomes sufficiently nonlinear (>5% deviation from linear fit), the spring is assumed to have plastically deformed, thus setting an upper-bound on spring range-of-motion and gripper stroke.

The frictional resistance inherent to the castellated hinge joints (due to stiffness of the Kapton, the presence of residual adhesive in the vicinity, etc.) is currently unknown, so the stiffer spring with the behavior shown Figure 10 was employed in the prototype design to provide sufficient restoring force against this hinge frictional component.

MICROSURGICAL GRIPPER DESIGN & FABRICATION

An exploded CAD model of the gripper prototype, implementing the flexural return spring described above, is shown in Figure 11. The entire structure consists of 11 layers, with 304 Stainless Steel sheet stock (51 μm thick) as the structural material and 25 μm thick Kapton polyimide film as the flexible material.

The gripper was fabricated using the manufacturing process outlined in a previous section. The manufactured gripper in its 'un-popped' (post-release) configuration is shown in Figure 12. By folding up the notched flaps on the structural end of the gripper (the right half), the notches on the bottom layer fit into the slots on the top layer, locking the gripper into its fully-assembled (popped) configuration. Solder or a contact adhesive can be applied to these interfaces to fix the gripper in this

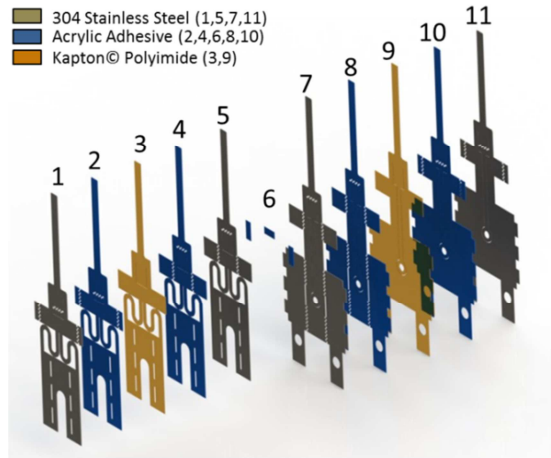


Figure 11: Exploded assembly rendering of gripper prototype

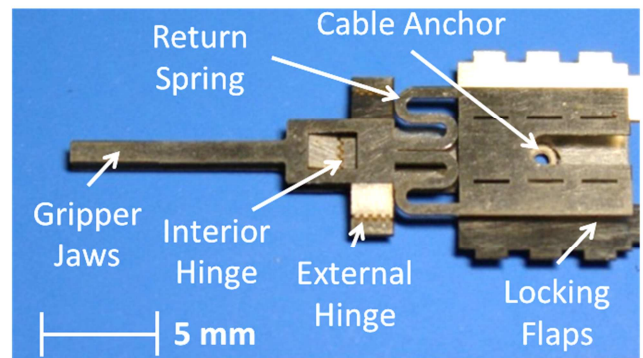


Figure 12: Un-popped gripper prototype with feature callouts

configuration. A drawbeam is machined directly into the bottom layer with an alignment interface for installation of cabling, which when pulled actuates the foremost interior hinge to close the gripper. Two external hinges constrain any transverse movement between upper and lower gripper jaws so that a pure closing motion is achieved.

An image of the 'popped-up' gripper manipulating a 19mm, 1.5-gauge (m) straight-taper suture needle is shown Figure 13.

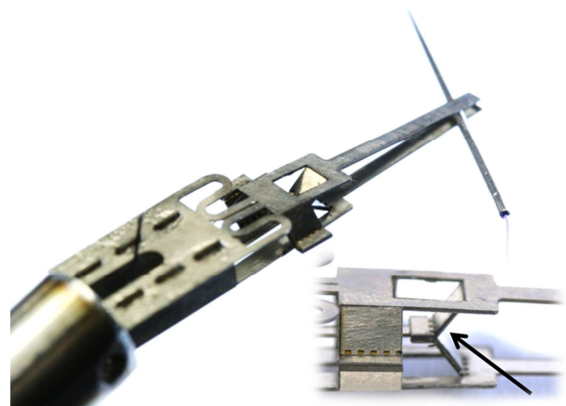


Figure 13: Gripper prototype manipulating a suture needle, (inset) close-up of gripper interior actuation hinge

The gripper is capable of full closure when actuated by the cable attached to the interior hinge. As designed, the gripper returns to an 'open' position when actuation load is removed. As can be seen, the stiffness of the spring is large enough such that the gripper approximates an 'alligator' closing motion typical of commercially-available forceps and grippers.

Benchtop tests were performed where the gripper was actuated to grasp and lift sequentially increasing, calibrated weights. The gripper can manipulate steel weights up to 20g, which is roughly 100 times its own weight of 200 milligrams. The grip force upper limit is set by a poor friction interface between the gripper and the object, as well as compliance in the gripper jaws given the 10:1 length-to-width aspect ratio.

CONCLUSIONS

In this paper, we have established the utility of Pop-Up Book MEMS fabrication for the development of medical devices by demonstrating that these devices can tolerate significant forces before failure, including joint shear stresses of $26.8 \pm 0.53 \text{ N/mm}^2$ and hinge torques of $22.8 \pm 2.15 \text{ N}\cdot\text{mm}$ per mm of hinge width. Failure behaviors were shown to be very predictable with no incidence of statistical outliers. Strength quantities determined from this evaluation will be used to create scaling laws to aid in the design of future Pop-Up microdevices.

In addition to the robustness evaluation, we designed and fabricated a gripper prototype with active cable-driven clamping and passive flexure-driven opening. The gripper operated as designed and was able to manipulate objects 100 times its own weight, further demonstrating the value of the Pop-Up fabrication process for microsurgical instrument development. Successful demonstration of this device provides a springboard for future medical device development using Pop-Up book MEMS.

Future work will include the investigation of effects of manufacturing process variations on mechanical robustness in an effort to streamline and simplify the fabrication process. Biocompatibility of composite materials will also be studied in a simulated *in vivo* environment. In order to comply with the design requirements set forth in [13], parallel-closing gripper jaws are required, so further work is necessary to design a spring with the required compliance such that parallel closure can be achieved. We will investigate the feasibility of directly machining surface features into the jaws, implementing high-friction rubber coatings, and implementing embedded jaw stiffness features to improve clamping force performance. With these improvements, we predict an overall improvement of gripper jaw clamping force, and a more robust mechanism overall. The gripper will also be outfitted with sensors to measure force and other physiological signals and be suitable for integration with the robotic system discussed in [13] to realize a force-feedback teleoperative microsurgical system.

REFERENCES

- [1] R. Berger, "Small-Joint Arthroscopy in the Hand and Wrist," in *Wrist Arthroscopy*, New York, Springer, 2005, pp. 155-166.
- [2] U. Seibold, B. Kuebler, H. Weiss, T. Ortmaier and G. Hirzinger, "Sensorized and Actuated Instruments for Minimally Invasive Robotic Surgery," in *EuroHaptics*, Munic, Germany, 2004.
- [3] W. Chang and D. Sretavan, "Microtechnology in Medicine: The Emergence of Surgical Microdevices," *The Congress of Neurological Surgeons*, vol. 54, pp. 137-47, 2007.
- [4] M. Murali and S. Yeo, "Rapid Biocompatible Micro-Device Fabrication by Electro-Discharge Machining," *Biomedical and Microdevices*, 2004.
- [5] J. B. Gafford, M. A. Cullinan, R. M. Panas and M. L. Culpepper, "Design Principles and Best-Practices for Rapid Prototyping Mesoscale Nanopositioners using a Micromill," in *ASPE Annual Meeting*, Atlanta, GA, 2010.
- [6] J. Whitney, P. Sreetharan, K. Ma and R. Wood, "Pop-Up Book MEMS," *J Micromech. Microeng.*, vol. 21, no. 115021, 2011.
- [7] P. Sreetharan, J. Whitney, M. Strauss and R. Wood, "Monolithic Fabrication of Millimeter-Scale Machines," *J. Micromech. Microeng.*, vol. 22, no. 055027, 2012.
- [8] N. Inagaki, "Plasma Graft Copolymerization," in *Materials Surface Processing by Directed Energy Techniques*, Oxford, UK, Elsevier, 2006, pp. 702-07.
- [9] "ASTM D1002-10: Standard Test Method for Apparent Shear Strength of Single-Lap-Joint Adhesively Bonded Metal Specimens by Tension Loading (Metal-to-Metal)," in *ASTM Standard Tensile Testing Protocol*.
- [10] N. Draper and H. Smith, *Applied Regression Analysis*, New York - London - Sydney: John Wiley and Sons, Inc., 1966.
- [11] Y. Lin, H. Liu and H. Chen, "Surface Modification of Polyimide Films by Argon Plasma," *Journal of Applied Polymer Science*, vol. 9, no. 3, pp. 744-55, 2005.
- [12] M. Mantel and J. Wightman, "Influence of the Surface Chemistry on the Wettability of Stainless Steel," *Surface and Interface Analysis*, vol. 21, pp. 595-605, 1994.
- [13] F. Hammond III, R. Kramer, Q. Wan, R. Howe and R. Wood, "Soft Tactile Sensors for Micromanipulation," in *Proc. of 2012 IEEE Int. Conf. on Intelligent Robotics and Systems*, Vilamoura, Portugal, 2012.
- [14] G. Barillaro, A. Molfese, A. Nannini and F. Pieri, "Analysis, Simulation, and Relative Performances of Two Types of Serpentine Springs," *J. Micromech. Microeng.*, vol. 15, pp. 736-746, 2005.